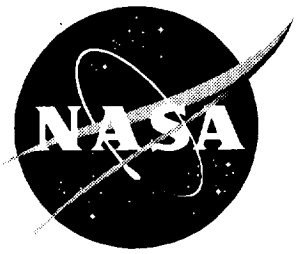
NASA/TP-1999-209320



Contribution of High Charge and Energy (HZE) Ions During Solar-Particle Event of September 29, 1989

Myung-Hee Y. Kim and John W. Wilson
Langley Research Center, Hampton, Virginia

Francis A. Cucinotta
Johnson Space Center, Houston, Texas

Lisa C. Simonsen
Langley Research Center, Hampton, Virginia

William Atwell
Boeing North American, Houston, Texas

Francis F. Badavi
Christopher Newport University, Newport News, Virginia

Jack Miller
Lawrence Berkeley National Laboratory, Berkeley, California

National Aeronautics and
Space Administration

Langley Research Center
Hampton, Virginia 23681-2199

May 1999

Available from:

NASA Center for AeroSpace Information (CASI)
7121 Standard Drive
Hanover, MD 21076-1320
(301) 621-0390

National Technical Information Service (NTIS)
5285 Port Royal Road
Springfield, VA 22161-2171
(703) 605-6000

Symbols

BFO	blood forming organ
C	coefficient (see eq. (3))
CAM	computerized anatomical man
CRT	cosmic ray telescope
DFE	degree of iron (FE) enhancement
E	kinetic energy, MeV/amu
GOES	Geostationary Operational Environmental Satellite
GSFC	Goddard Space Flight Center
H	dose equivalent, cSv
HZE	high charge and energy
IMP	Interplanetary Monitoring Platform
LET	linear energy transfer
NCRP	National Council on Radiation Protection and Measurements
$p(E)$	momentum, $\sqrt{E(E+1876)}$
p_{30}	momentum corresponding to proton energy of 30 MeV, 239.15 MV
$SEPB_Z$	solar energetic particle baseline for atomic charge
SPE	solar-particle event
VLET	very low energy telescope
Z	atomic charge
$\alpha(E)$	enhancement index
β	proton velocity relative to velocity light
Φ	integral fluence, particles/cm^2
$\phi_p(E)$	differential fluence, protons/(cm^2-MeV)
$\phi_Z(E)$	energy spectra of atomic charge

Abstract

The solar-particle event (SPE) of September 29, 1989, produced an iron-rich spectrum with energies approaching 1 A GeV with an approximate spectral slope parameter of 2.5. These high charge and energy (HZE) ions challenge conventional methods of shield design and assessment of astronaut risks. In the past, shield design and risk assessment have relied on proton shielding codes and biological response models derived from X-ray and neutron exposure data. Because the HZE spectra decline rapidly with energy and HZE attenuation in materials is limited by their penetration power, details of the mass distributions about the sensitive tissues (shielding materials and the astronaut's body) are important determining factors of the exposure levels and distributions of linear energy transfer. Local tissue environments during the SPE of September 29, 1989, with its HZE components are examined to analyze the importance of these ions to human SPE exposure. Typical space suit and lightly shielded structures leave significant contributions from HZE components to certain critical body tissues and have important implications on the models for risk assessment. A heavily shielded equipment room of a space vehicle or habitat requires knowledge of the breakup of these ions into lighter components, including neutrons, for shield design specifications.

Introduction

Solar-particle events (SPE's) have long been recognized as a potential hazard to human operations in space. Recently, the SPE of August 4–7, 1972, was analyzed, and the inclusion of dose rate effects on risk assessment was found to reduce health effects of exposure by a factor of 3 in comparison with a single high-dose-rate exposure (ref. 1). In that calculation, only incident protons were considered, as that was the data set available for analysis. A large SPE, occurring on September 29, 1989, contained an iron-rich spectrum with energies approaching 1 A GeV and an approximate energy power index of 2.5 (ref. 2). This SPE is the largest high-energy event of the space era (1959 to present), and 10 times this event matches the ground level data of the SPE of February 23, 1956. It suggests a 10-scaled event as a worst case event for a design guide of future deep space mission.

To analyze the importance of HZE ions to human SPE exposure and for a design guide for future deep space missions, the event-integrated fluences of the SPE of September 29, 1989, are constructed from the limited measured data. The proton spectrum above 30 MeV is well described by a model developed by Nymmik (refs. 3 and 4). Below that energy, an exponential distribution of protons developed by Shea and Smart is used (ref. 5). The enhancements of the high charge and energy (HZE) ion abundances, which may present new and significant problems for radiation protection, are calculated relative to solar energetic particle baseline (SEPB) abundances (ref. 6). By using the HZETRN code systems (ref. 7), transport properties of the shielding materials and an astronaut's body tissues are calculated. The typical shield configurations are assumed to be equivalent aluminum structures. The astronaut geometry is taken from the computerized anatomical man (CAM) model (ref. 8). The risk assessment and the risk contributions of particle groups are made with the full spectrum of the SPE of September 29, 1989, to characterize local tissue environments.

Energy Spectra of SPE of September 29, 1989

Analytic representation of proton spectra is made according to the model of Nymmik (refs. 3 and 4) for energies above 30 MeV and the exponential rigidity spectra of Shea and Smart (ref. 5) for energies below 30 MeV. From the model of Nymmik (refs. 3 and 4), the event-integrated proton fluence above 30 MeV of this event is given by

$$\int_{30}^{\infty} \phi_p(E)\, dE = 1.39 \times 10^9 \text{ protons/cm}^2 \quad (1)$$

where E is the kinetic energy, and $\phi_p(E)$ is the differential fluence. For the proton differential fluence above 30 MeV, $\phi_p(E)$ is given as a power law by

$$\phi_p(E)\,dE = \frac{C}{\beta} \times \left[\frac{p(E)}{p_{30}}\right]^{-4.5} dE \qquad (2)$$

where β is the proton velocity relative to the velocity of light, the momentum $p(E) = \sqrt{E(E+1876)}$, and p_{30} is the momentum corresponding to a proton energy of 30 MeV, which is equivalent to 239.15 MV. The coefficient C is calculated from equation (2) as

$$C = \frac{1.39 \times 10^9}{\int_{30}^{\infty} \left[\frac{239.15}{p(E)}\right]^{4.5} \frac{1}{\beta}\,dE} = 2.034 \times 10^7 \qquad (3)$$

The differential fluence below 30 MeV is calculated by using an exponential distribution (ref. 5) because there is a flattening of the spectra below 30 MeV based upon observations of this event (ref. 9). This calculation gives a very good empirical description of data below 30 MeV, and the integral energy spectra above 1 MeV of this event are well described with measured data of NOAA (ref. 10) as shown in figure 1.

Empirical representations of oxygen and iron spectra are given by Tylka, Dietrich, and Boberg (ref. 2) as shown in figures 2 and 3. In these figures, the mean spectral slopes are 3.9 and 2.5 for oxygen and iron particles, respectively. To obtain the abundance distributions from He to Ni (Z = 2 to 28), oxygen is chosen as the element for the SEPB to which the relative abundances of those ions are normalized because its statistics are the best for the ions heavier than He (ref. 6). The defined SEPB values in reference 6 are reproduced in table 1, with which the energy spectra from He to N (Z = 2 to 7) are given as

$$\phi_Z(E) = \mathrm{SEPB}_Z \times \phi_O(E) \qquad (4)$$

where $\phi_O(E)$ is the energy spectra of oxygen.

In some events, an enhancement of heavy ion abundances is seen relative to an SEPB that increases with increasing atomic number. These enhancements have some correlation with spectral slope (ref. 6). The SEPB Fe/O ratio is 0.066, but for the SPE of September 29, 1989, the fluence ratio for Fe/O is approximately 0.2, which demonstrates that this event is enriched in Fe threefold. This enhancement is viewed as a distinct physical process superposed on some underlying pattern for ions heavier than oxygen, and their spectra are classified by the degree of Fe enhancement (DFE) with increasing atomic number Z beyond oxygen as follows:

$$\mathrm{DFE}(Z, E) = \left(\frac{Z}{8}\right)^{\alpha(E)} \qquad (5)$$

Here, the enhancement index $\alpha(E)$ is given from the energy spectra of oxygen and iron as

$$\alpha(E) = \frac{\ln\left[\frac{\phi_{Fe}(E)}{\phi_O(E)}\left(\frac{1}{0.066}\right)\right]}{\ln\left(\frac{26}{8}\right)} \qquad (6)$$

The degree of enhancement at 100 A MeV of each atomic charge number beyond oxygen (eq. (5)) is shown in figure 4 for its abundance relative to the baseline abundance. With the degree of enhancements and the SEPB abundances, the data for ions from F to Mn (Z = 9 to 25) are obtained as

$$\phi_Z(E) = \mathrm{SEPB}_Z\ \phi_O(E) \left(\frac{Z}{8}\right)^{\alpha(E)} \qquad (7)$$

For Co (Z = 27) and Ni (Z = 28) energy spectra, one thirtieth and one tenth of Fe ion spectra are taken, respectively, which are the relative abundances in cosmic ray fluence. The relevant integrated fluence spectra of the SPE of September 29, 1989, are shown in figure 5. These spectra are used as input to the transport code systems, HZETRN (ref. 7), for the risk analysis of the SPE of September 29, 1989.

Critical Regions Considered Inside Shield for SPE Protection

Particles arriving at some remote location from the Sun are diffusing through the interplanetary media and show some anisotropy because in the leading edge of the expanding radiation field, back-scattered particles are absent. Following the first 20 to 30 min after initial particle arrival, isotropy is usually achieved; therefore, the radiation fields that are incident on the spacecraft are assumed to be isotropic. Simple spacecraft geometry is chosen in which an astronaut is

assumed to be at the center of a large spherical shell of uniform material. Three typical shield representations for a spacecraft are space suit, pressure vessel, and equipment room. These shields are assumed as equivalent aluminum structures: space suit with a thickness of 0.3 g/cm^2, pressure vessel with a thickness of 1 g/cm^2, and equipment room with a thickness of 5 g/cm^2 (ref. 11).

Inside a shield enclosure, three critical organs considered in this study are skin, ocular lens, and blood forming organ (BFO). In order to determine spatially the positions of these critical sites, the computerized anatomical man (CAM) model, which contains 2400 separate geometric tissue regions of several different elemental compositions and densities (ref. 8), is used. The detailed mass distributions of body geometry from 512 rays are used to generate fluences of the various components of solar particles at each site inside a shield.

Risk Assessment at Local Tissue Environment

The incident fluences from the SPE of September 29, 1989, inside typical space shields are calculated with the HZETRN code system (ref. 7). The interior radiation environment is transported through the inhomogeneous and geometrically complex body to calculate the specific local tissue environment. The radiation risks in terms of conventional dosimetry, dose and dose equivalent with quality factor (ref. 12), are estimated at local tissue environments. These are shown in tables 2 and 3.

The dose equivalent contributions of particle groups to the skin inside shields are shown in figure 6. Skin is the least dependent on individual body masses, and the fractional contribution of protons increases as a function of equivalent aluminum shielding because of the breakup of multiple charged ions and secondary production from HZE nuclear interactions with mainly shield materials, as evident from figure 6. At the ocular lens, the fractional contributions of all the particle groups show the same trend as for skin but with a lesser degree of change as shown in figure 7. This trend is caused by an increased shielding by body masses than for skin. The fractional contributions of all the particle groups at BFO are nearly independent of the shield thickness as shown in figure 8. It is reasoned that BFO is the most dependent on individual body masses and all the radiation components are attenuated to some degree (ref. 13) before reaching the specific target site of BFO. The most body-shielding effect is achieved at BFO among the sensitive sites considered. The risk contribution is further analyzed to study the detailed local tissue environment and is presented as follows.

The differential spectra of dose equivalents in figures 9 through 11 show the detailed risks calculated for local tissue environments. In these figures, the height of each curve is proportional to the contribution for that energy interval. At skin and ocular lens within a shield, most HZE particles have not reached the end of their range, but after passing through a shield and body masses they have been slowed down to higher LET and fragmented into smaller HZE's that have higher quality factors. At BFO, which is rather deep into the body, most HZE particles have been substantially stopped. The energy levels at the peak contribution of dose equivalent are shifted to higher energy levels for all the particle groups, as the sensitive site shifts to deeper within the body. This change is because HZE particles with high penetration power become the most effective radiation constituent at that location. Also noticeable are still significant risk contributions from HZE particles to these tissues inside a space suit and pressure vessel, as shown in figures 9 and 10.

In figures 9 through 11, two sources of secondary particles for atomic charge number 1 and 2 are identified. Differential dose equivalent contributions at low energy correspond to targetlike fragments, and those at high energy are from projectilelike fragments (ref. 14). Relatively abundant low-energy protons and alpha particles have been produced by nuclear interactions of all primaries in shielding materials and body, and they contribute substantially to the calculated dose equivalent. Detailed local tissue environments are determined by the mass distributions of shielding materials and body geometry.

In table 3, dose equivalent calculations of the SPE are given along with the NCRP 30-day limit (ref. 15). These limits are set to preclude both acute and late nonstochastic effects by not exceeding the threshold levels to these effects. From the table, total dose equivalent at each local tissue is significantly reduced

as shield thickness is increased from space suit, to pressure vessel, and to equipment room. But dose equivalent in the equipment room only is within the acceptable NCRP 30-day limit at each local tissue. Therefore, only the equipment room provides sufficient shielding to avoid acute or nonstochastic late effects in sensitive organs by the NCRP 30-day limit.

For the current risk estimation, the dose equivalent is calculated by using the defined quality factors (ref. 12). These quality factors are derived principally for carcinogenesis and mutagenesis, and the actual risk estimates for acute exposure may be somewhat lower than the current estimation. The current estimation is approximated at best, since quality factors for early radiation effects are not defined (ref. 12). Furthermore, not only track structure effects on injury cross sections are poorly understood, but there is a lack of detailed spectral data for alpha particles and heavier ions emitted during the SPE. Because the full heavy ion spectra of the SPE of September 29, 1989, are constructed from the limited measured data, the current risk estimation for this SPE will be changed undoubtedly due to these uncertainties.

The current risk estimation in table 3 shows that skin dose equivalent inside a space suit would be very large (≈300 Sv) for an event of similar spectral characteristics and 10 times intensities of the SPE of September 29, 1989, such as the SPE of February 23, 1956. Even a dose rate reduction factor of 2 to 3 (ref. 1) would leave the exposures high compared with the threshold for moist desquamation of 30 Gy (30 Sv) for gamma rays (ref. 15). The mortality threshold is 1.5 Gy (1.5 Sv) for gamma rays, which is much lower than 4.2 Sv to BFO inside a space suit for a "February 23, 1956 SPE." In addition to the possibility of skin infection with an already depressed immune system, the coincident BFO exposure may provide a serious medical problem to the astronauts. Clearly, more shielding is required even within an equipment room to protect the critical tissues during most of SPE's. An understanding of the breakup of HZE ions into lighter components, including neutrons, is required for shield design specification because all HZE particles are not stopped as has been shown in figures 9 through 11. The buildup of neutrons is harmful even inside an equipment room because they are an important source of the proton and He ion exposures within the tissues. Indeed, for the contributions of dose equivalents of $Z = 1$ and 2 at low energy near 0.1 to several MeV/amu, these particles result from neutrons produced in the shielding materials.

Concluding Remarks

The event-integrated fluences of the solar-particle event (SPE) of September 29, 1989, are calculated according to the descriptions of the observed spectra. This SPE was threefold enriched in Fe relative to the baseline composition of SPE. The risk estimations clearly show that critical organs respond differently to their local environments. To obtain accurate local tissue environments, the detailed mass distributions of shielding materials and the sensitive tissues are required, and they are important determining factors for accurate exposure level assessments and linear energy transfer (LET) distributions. The result shows that high charge and energy (HZE) ions play a limited role inside a lightly shielded space suit and for the least shielded organs by the NCRP 30-day limit during the SPE of September 29, 1989.

The detailed risk analysis according to the differential spectra of dose equivalent shows that even a heavily shielded equipment room cannot stop completely all energetic particles, which may break up into lighter components including neutrons from the body. Therefore, a well-shielded region and medical treatment must be considered when a large SPE occurs during deep space mission.

For accurate risk estimations and shield design specifications, the spectral data for alpha particles and heavier ions emitted during SPE's are required as well as quality factors for early radiation effects. Improved understanding of track structure effects on injury cross sections and accurate nuclear databases including neutrons are required to decrease the risk estimate uncertainties.

References

1. Wilson, John W.; Shinn, Judy L.; Simonsen, Lisa C.; Cucinotta, Francis A.; Dubey, R. R.; Jordan, W. R.; Jones, T. D.; Chang, C. K.; and Kim, M. Y.: *Exposures to Solar Particle Events in Deep Space Missions.* NASA TP-3668, 1997.

2. Tylka, Allan J.; Dietrich, William F.; and Boberg, Paul R.: High-Energy Solar Heavy Ions From IMP-8. Naval Res. Lab. paper presented at Workshop on Impact of Solar Energetic Particle Events for Design of Human Missions, Center for Adv. Sp. Studies (Houston, TX), Sept. 9–11, 1997.

3. Nymmik, Rikho: Probabilistic Model for Fluences and Peak Fluxes of Solar Particles. Moscow State Univ. paper presented at Workshop on Impact of Solar Energetic Particle Events for Design of Human Missions, Center for Adv. Sp. Studies (Houston, TX), Sept. 9–11, 1997.

4. *Space Environment (Natural and Artificial) Probabilistic Model for Fluences and Peak Fluxes of Solar Cosmic Ray Particles.* ISO WD 15391, Int. Org. Stand. http://www.npi.msu.su/scrf/standart/ISO_WD_15391.html Accessed Feb. 11, 1999.

5. Shea, M. A.; and Smart, D. F.: A Summary of Major Solar Proton Events. *Solar Phys.*, vol. 127, June 1990, pp. 297–320.

6. McGuire, R. E.; and Von Rosenvinge, T. T.: The Composition of Solar Energetic Particles. *Astrophys. J.*, vol. 301, Feb. 1986, pp. 938–961.

7. Wilson, John W.; Badavi, Francis F.; Cucinotta, Francis A.; Shinn, Judy L.; Badhwar, Gautam D.; Silberberg, R.; Tsao, C. H.; Townsend, Lawrence W.; and Tripathi, Ram K.: *HZETRN: Description of a Free-Space Ion and Nucleon Transport and Shielding Computer Program.* NASA TP-3495, 1995.

8. Atwell, William; Weyland, Mark D.; and Simonsen, Lisa C.: Solar Particle Dose Rate Buildup and Distribution in Critical Body Organs. *Biological Effects and Physics of Solar and Galactic Cosmic Radiation.* Part B, Charles E. Swenberg, Gerda Horneck, and E. G. Stassinopoulos, eds., Plenum Press, 1993, pp. 831–844.

9. Cleghorn, Timothy F.; and Badhwar, Gautam D.: Comparison of the SPE Model With Proton and Heavy Ion Data. NASA paper presented at Workshop on Impact of Solar Energetic Particle Events for Design of Human Missions, Center for Adv. Sp. Studies (Houston, TX), Sept. 9–11, 1997.

10. Sauer, Herbert H.; Zwickl, Ronald D.; and Ness, Martha J.: *Summary Data for the Solar Energetic Particle Events of August Through December 1989.* Space Environment Lab., National Oceanic and Atmospheric Adm., 1990.

11. Wilson, J. W.; and Denn, F. M.: *Preliminary Analysis of the Implications of Natural Radiations on Geostationary Operations.* NASA TN D-8290, 1976.

12. *1990 Recommendations of the International Commission on Radiobiological Protection.* ICRP Publ. 60, Pergamon Press Inc., 1991.

13. Kim, Myung-Hee Y.; Wilson, John W.; Thibeault, Sheila A.; Nealy, John E.; Badavi, Francis F.; and Kiefer, Richard L.: *Performance Study of Galactic Cosmic Ray Shield Materials.* NASA TP-3473, 1994.

14. Cucinotta, Francis A.; Wilson, John W.; and Badavi, Francis F.: *Extension of the BRYNTRN Code to Monoenergetic Light Ion Beams.* NASA TP-3472, 1994.

15. National Council on Radiation Protection and Measurements: *Guidance on Radiation Received in Space Activities.* NCRP Rep. No. 98, July 1989

Table 1. Solar Energetic Particle Baseline

[From ref. 6]

Particle	$SEPB_Z$	Particle	$SEPB_Z$
H/O	3500 ± 500	Na/O	0.0083 ± 0.0015
He/O	53 ± 5	Mg/O	0.183 ± 0.010
Li/O	<0.001	Al/O	0.0115 ± 0.018
Be/O	$<5 \times 10^{-4}$	Si/O	0.147 ± 0.009
B/O	$<5 \times 10^{-4}$	P/O	0.0014 ± 0.0006
C/O	0.454 ± 0.018	S/O	0.0229 ± 0.0025
N/O	0.129 ± 0.008	Ar/O	0.0016 ± 0.0007
O/O	1.00 ± 0.031	Ca/O	0.0076 ± 0.0016
F/O	$<5 \times 10^{-4}$	(Ti+Cr)/O	0.0024 ± 0.0009
Ne/O	0.128 ± 0.008	Fe(group)/O	0.066 ± 0.006

Table 2. Dose for SPE of September 29, 1989

Atomic Charge	Dose, cGy, at—								
	Skin inside—			Ocular lens inside—			BFO inside—		
	Space suit	Pressure vessel	Equipment room	Space suit	Pressure vessel	Equipment room	Space suit	Pressure vessel	Equipment room
$Z = 1$	780.9	296.0	39.9	377.2	193.5	36.8	27.6	23.4	13.1
$Z = 2$	105.2	10.2	0.7	16.7	4.8	0.6	0.4	0.4	0.2
$3 \le Z \le 10$	2.9	0.3	≈ 0	0.5	0.1	≈ 0	≈ 0	≈ 0	≈ 0
$11 \le Z \le 20$	0.7	0.1	≈ 0	0.2	0.1	≈ 0	≈ 0	≈ 0	≈ 0
$21 \le Z \le 28$	0.3	0.1	≈ 0	0.1	≈ 0	≈ 0	≈ 0	≈ 0	≈ 0
Total	890.0	306.6	40.6	394.5	198.4	37.4	28.0	23.8	13.3

Table 3. Dose Equivalent for SPE of September 29, 1989

Atomic Charge	Dose, cGy, at—								
	Skin inside—			Ocular lens inside—			BFO inside—		
	Space suit	Pressure Vessel	Equipment Room	Space suit	Pressure Vessel	Equipment Room	Space suit	Pressure Vessel	Equipment Room
$Z = 1$	1738.3	553.7	57.7	668.1	317.8	50.1	37.8	31.4	16.8
$Z = 2$	1149.3	81.9	6.6	132.3	33.1	4.9	4.0	3.5	2.4
$3 \leq Z \leq 10$	53.2	5.3	0.2	9.3	2.4	0.2	0.1	0.1	≈ 0
$11 \leq Z \leq 20$	9.0	1.6	0.1	2.4	0.9	0.1	0.1	0.1	≈ 0
$21 \leq Z \leq 28$	2.4	0.8	0.2	1.0	0.5	0.1	0.1	0.1	≈ 0
Total	2952.2	643.1	64.7	813.1	354.7	55.4	42.2	35.1	19.3
NCRP 30-day limit (ref. 15)	150			100			25		

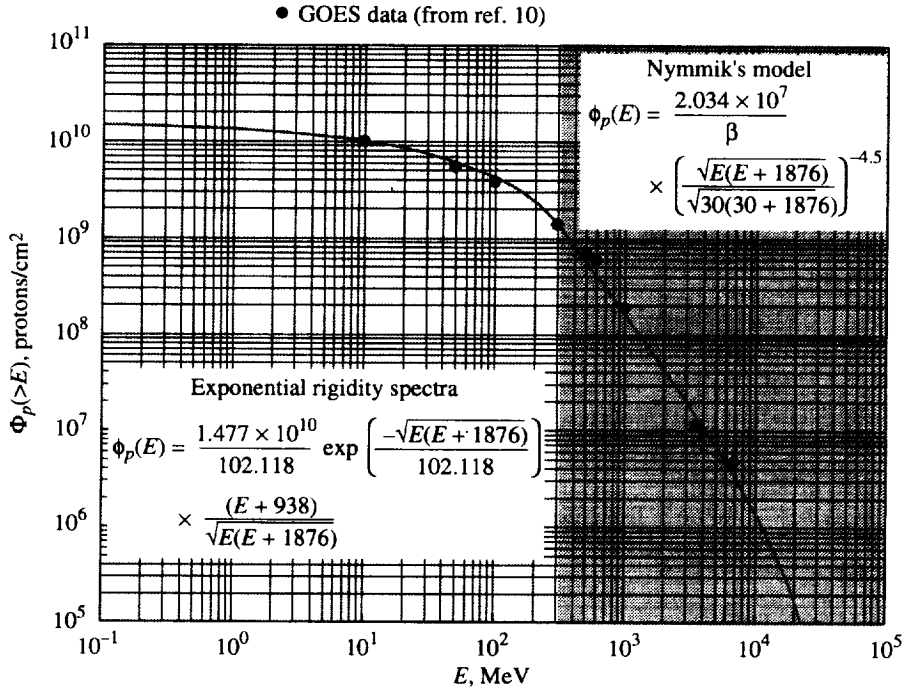


Figure 1. Analytic representation of proton spectra for SPE of September 29, 1989.

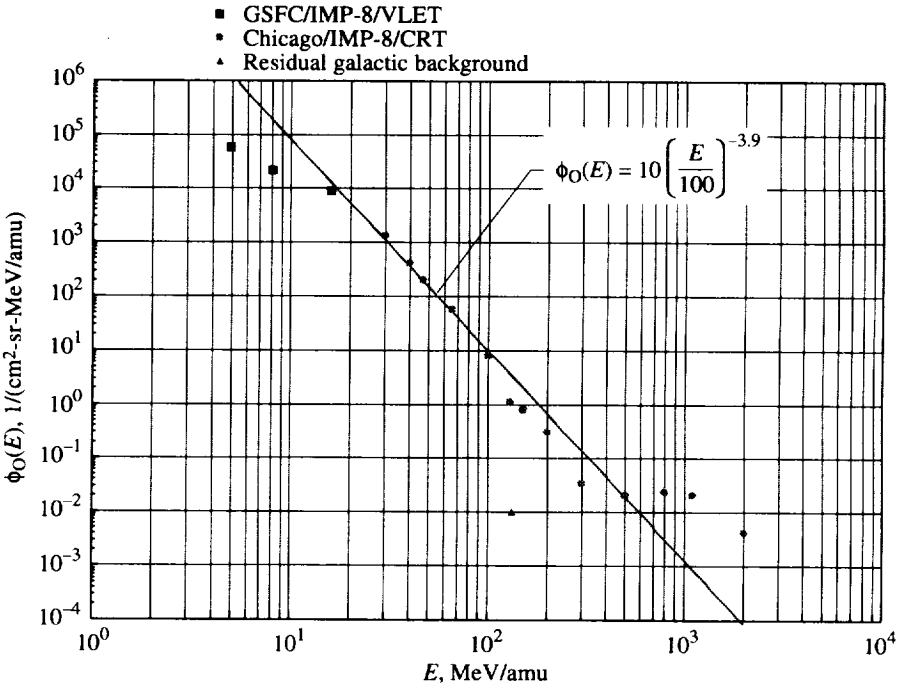


Figure 2. Empirical representation of oxygen spectra for SPE of September 29, 1989 (ref. 2).

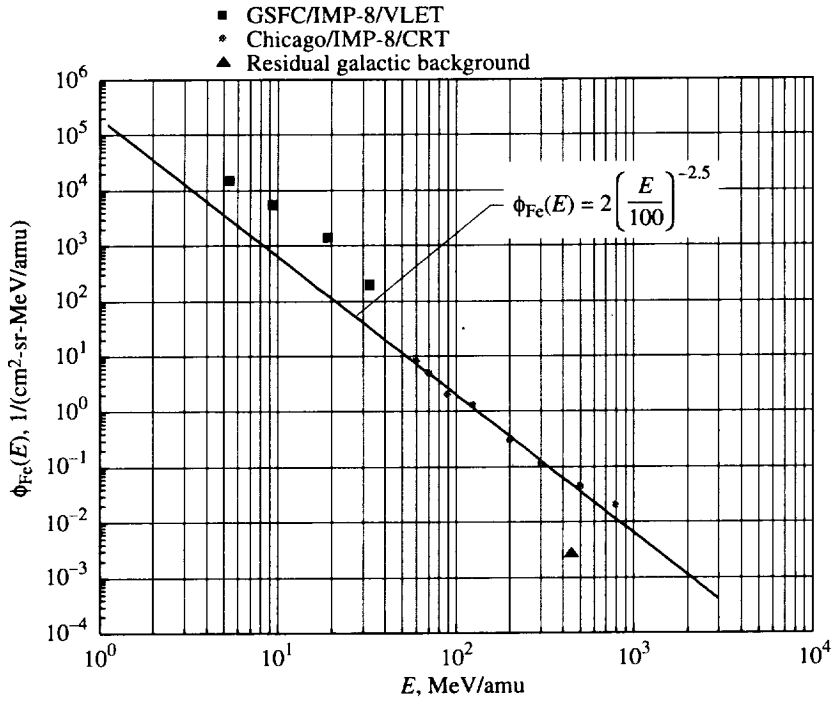


Figure 3. Empirical representation of iron spectra for SPE of September 29, 1989 (ref. 2).

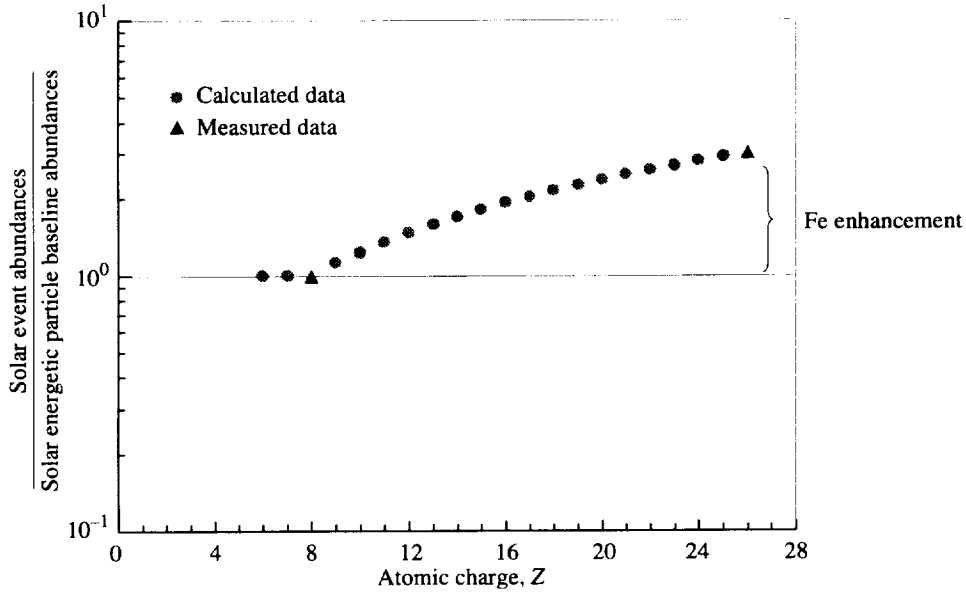


Figure 4. Prediction of September 29, 1989, solar event abundances relative to the SEPB abundances for each atomic charge number Z.

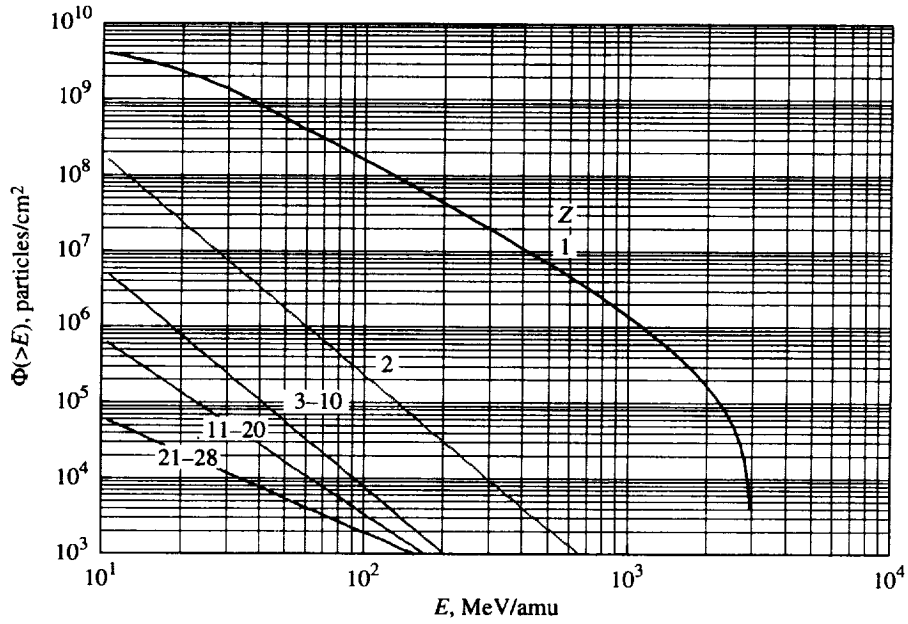


Figure 5. Event-integrated integral fluence spectra of SPE of September 29, 1989.

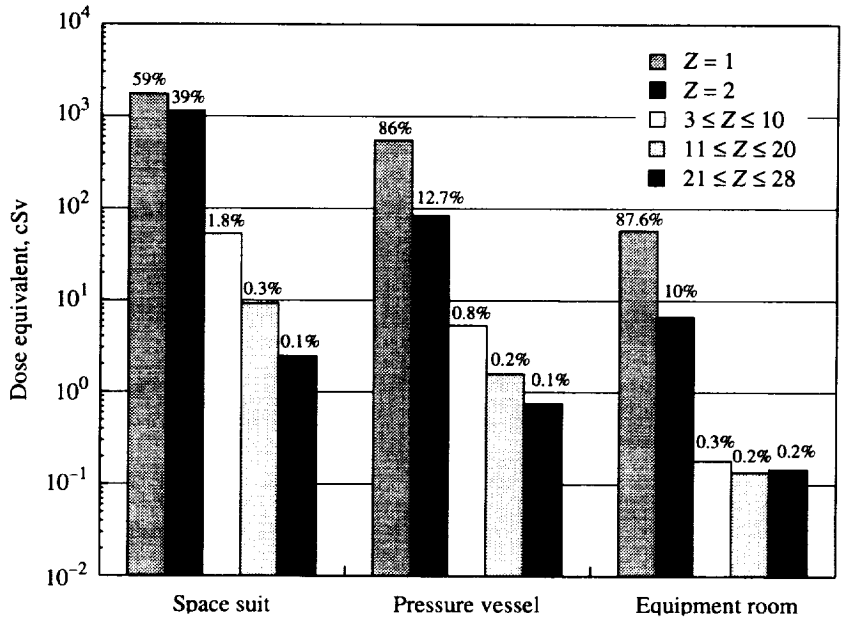


Figure 6. Dose equivalent at skin for SPE of September 29, 1989.

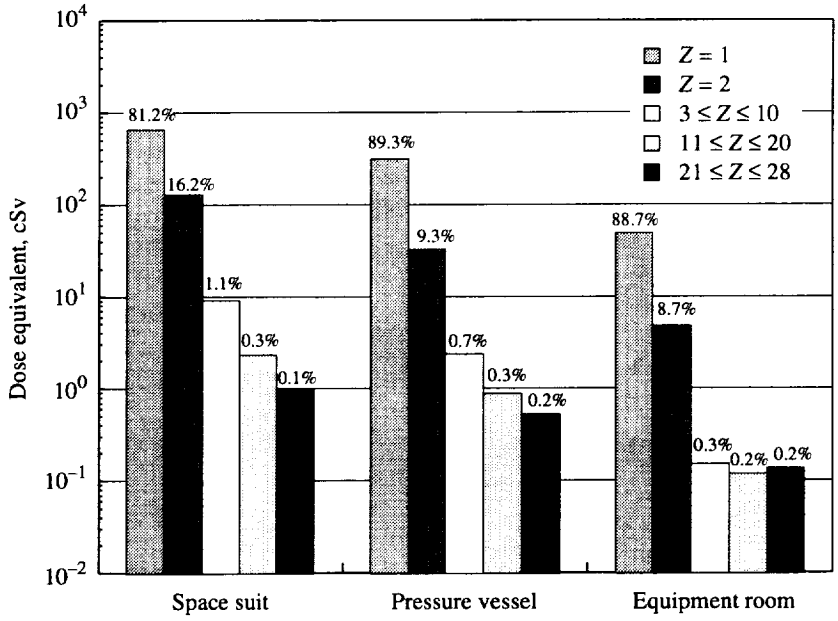


Figure 7. Dose equivalent at ocular lens for SPE of September 29, 1989.

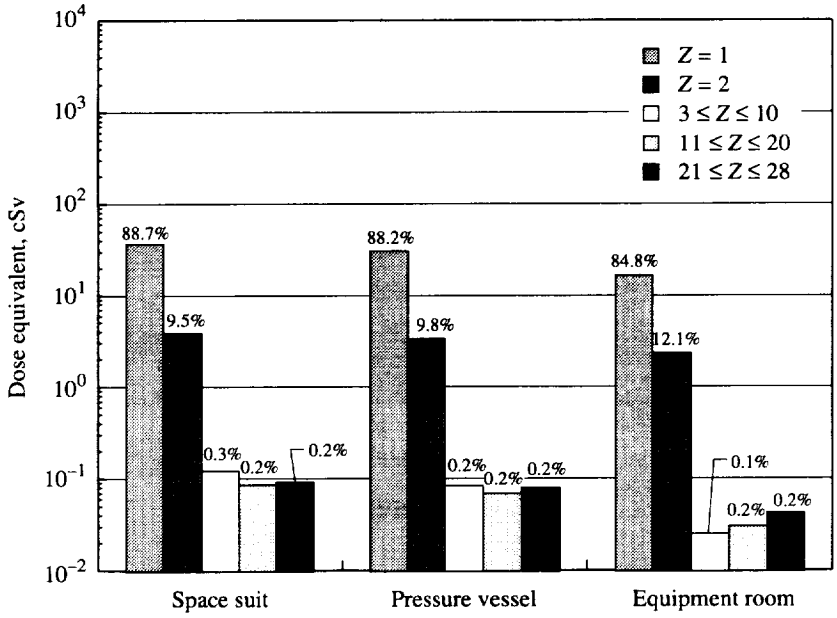
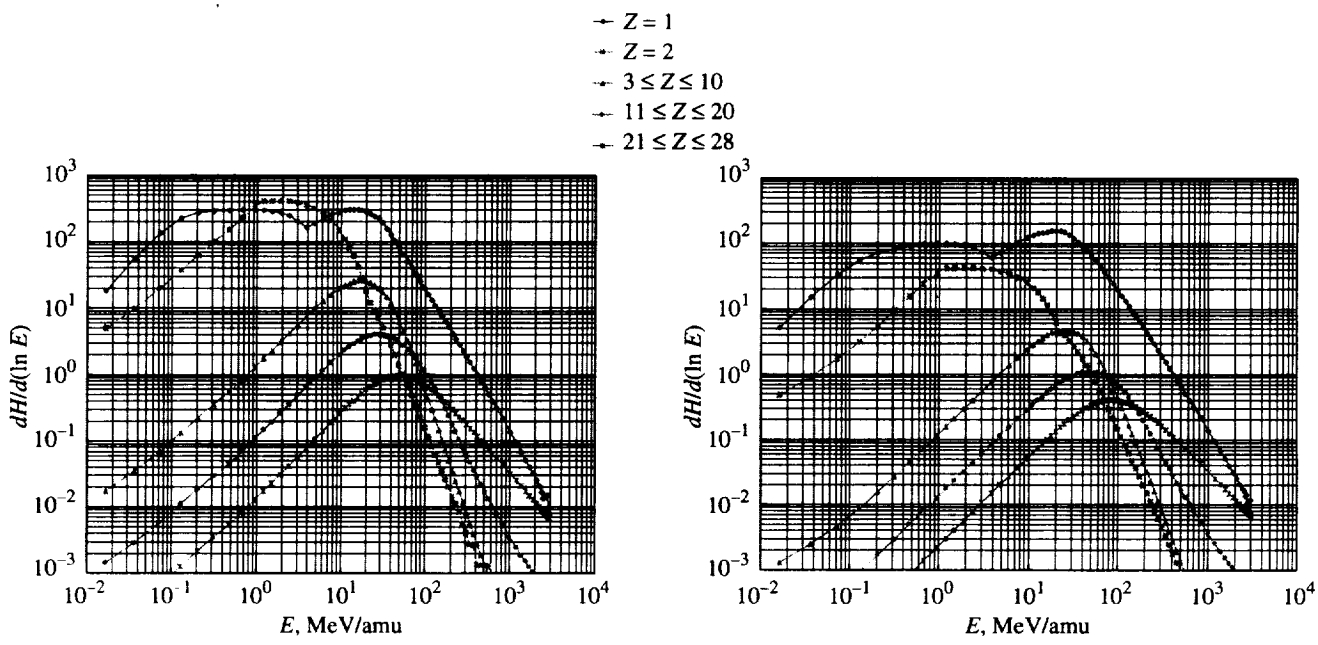
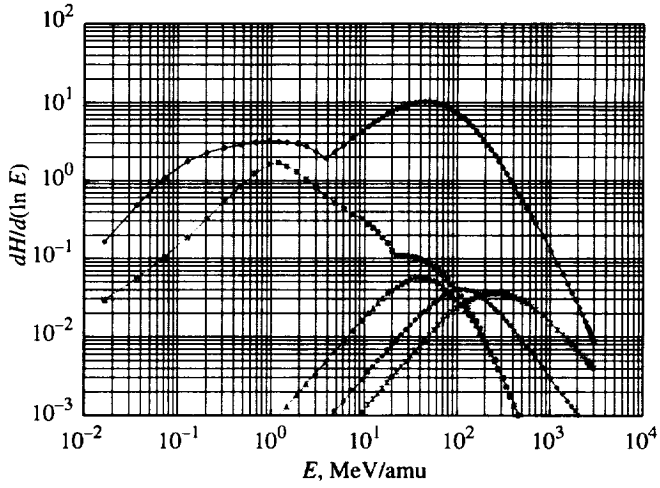


Figure 8. Dose equivalent at BFO for SPE of September 29, 1989.



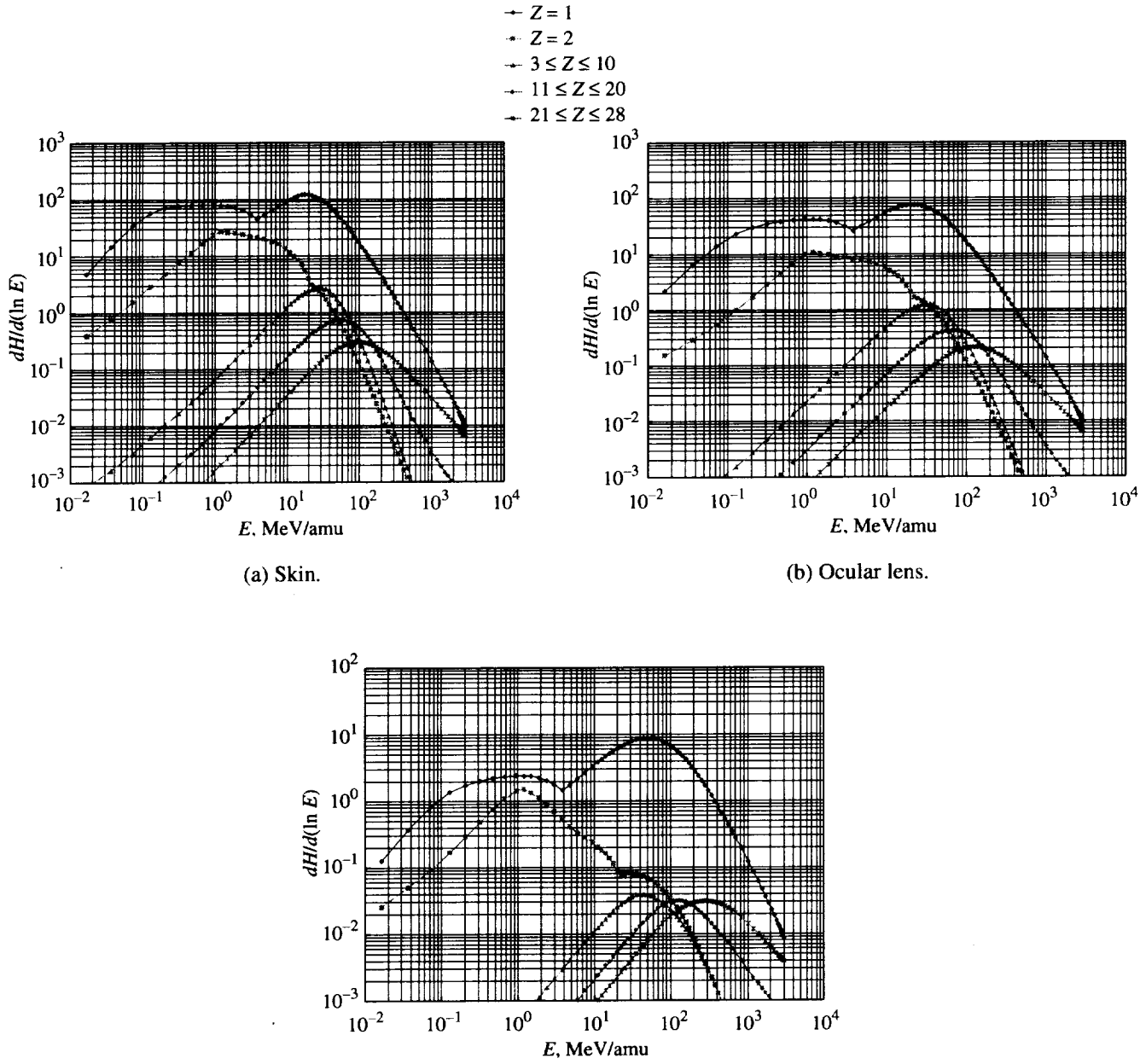
(a) Skin.

(b) Ocular lens.



(c) BFO.

Figure 9. Differential spectra of dose equivalent per logarithmic interval of energy per nucleon at different regions inside space suit.

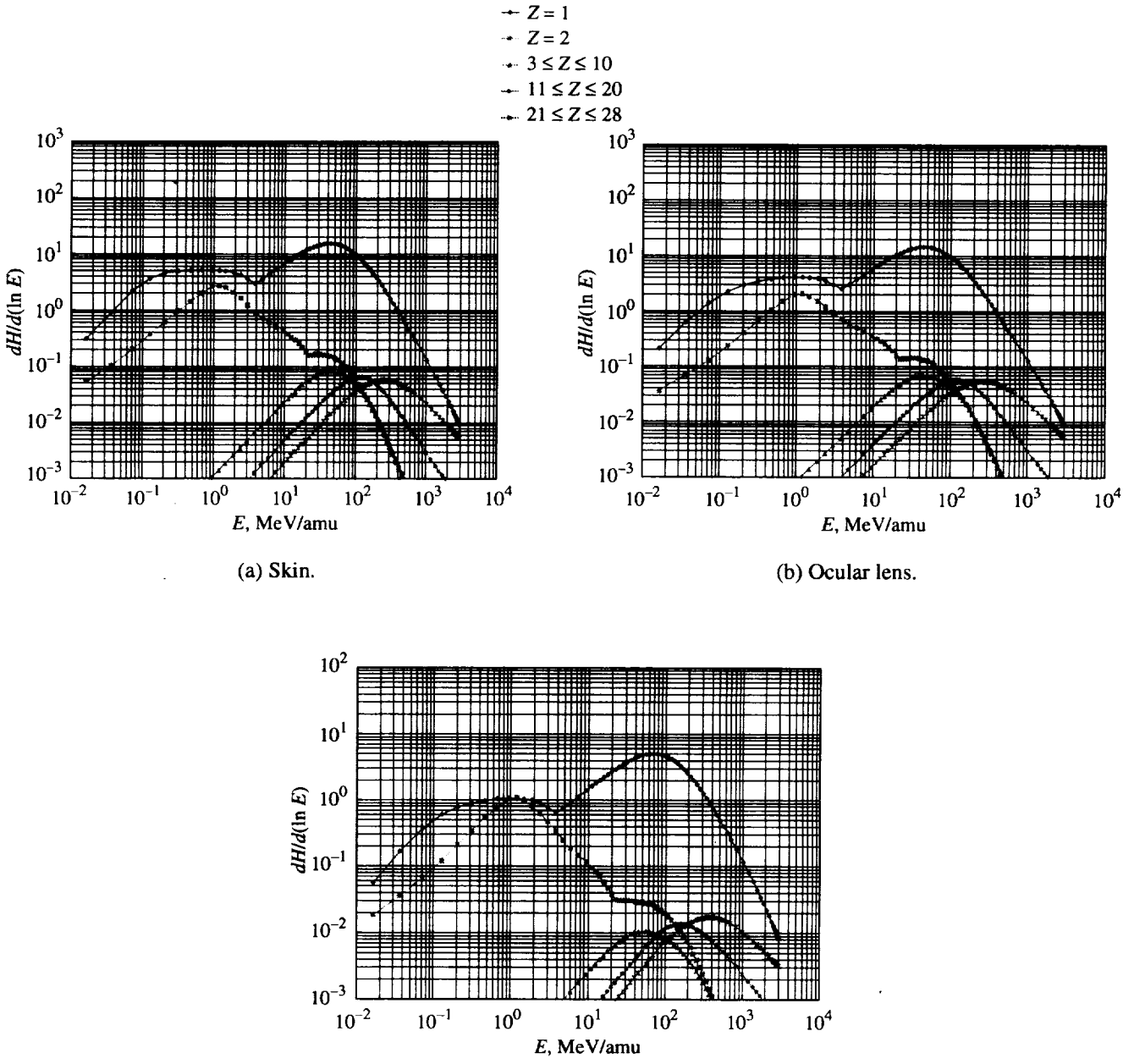


(a) Skin.

(b) Ocular lens.

(c) BFO.

Figure 10. Differential spectra of dose equivalent per logarithmic interval of energy per nucleon at different regions inside pressure vessel.



(a) Skin.

(b) Ocular lens.

(c) BFO.

Figure 11. Differential spectra of dose equivalent per logarithmic interval of energy per nucleon at different regions inside equipment room.

REPORT DOCUMENTATION PAGE

Form Approved
OMB No. 07704-0188

Public reporting burden for this collection of information is estimated to average 1 hour per response, including the time for reviewing instructions, searching existing data sources, gathering and maintaining the data needed, and completing and reviewing the collection of information. Send comments regarding this burden estimate or any other aspect of this collection of information, including suggestions for reducing this burden, to Washington Headquarters Services, Directorate for Information Operations and Reports, 1215 Jefferson Davis Highway, Suite 1204, Arlington, VA 22202-4302, and to the Office of Management and Budget, Paperwork Reduction Project (0704-0188), Washington, DC 20503.

1. AGENCY USE ONLY *(Leave blank)*	2. REPORT DATE	3. REPORT TYPE AND DATES COVERED
	May 1999	Technical Publication

4. TITLE AND SUBTITLE
Contribution of High Charge and Energy (HZE) Ions During Solar-Particle Event of September 29, 1989

5. FUNDING NUMBERS
WU 199-45-16-12

6. AUTHOR(S)
Myung-Hee Y. Kim, John W. Wilson, Francis A. Cucinotta, Lisa C. Simonsen, William Atwell, Francis F. Badavi, and Jack Miller

7. PERFORMING ORGANIZATION NAME(S) AND ADDRESS(ES)
NASA Langley Research Center
Hampton, VA 23681-2199

8. PERFORMING ORGANIZATION REPORT NUMBER
L-17744

9. SPONSORING/MONITORING AGENCY NAME(S) AND ADDRESS(ES)
National Aeronautics and Space Administration
Washington, DC 20546-0001

10. SPONSORING/MONITORING AGENCY REPORT NUMBER
NASA/TP-1999-209320

11. SUPPLEMENTARY NOTES
Kim: NRC-NASA Resident Research Associate at the Langley Research Center, Hampton, VA; Wilson and Simonsen: Langley Research Center, Hampton, VA; Cucinotta: Johnson Space Center, Houston, TX; Atwell, Boeing North American, Houston, TX; Badavi: Christopher Newport University, Newport News, VA; Miller: Lawrence Berkeley National Laboratory, Berkeley, CA.

12a. DISTRIBUTION/AVAILABILITY STATEMENT
Unclassified–Unlimited
Subject Category 93 Distribution: Standard
Availability: NASA CASI (301) 621-0390

12b. DISTRIBUTION CODE

13. ABSTRACT ***(Maximum 200 words)***

The solar-particle event (SPE) of September 29, 1989, produced an iron-rich spectrum with energies approaching 1 A GeV with an approximate spectral slope parameter of 2.5. These high charge and energy (HZE) ions challenge conventional methods of shield design and assessment of astronaut risks. In the past, shield design and risk assessment have relied on proton shielding codes and biological response models derived from X-ray and neutron exposure data. Because the HZE spectra decline rapidly with energy and HZE attenuation in materials is limited by their penetration power, details of the mass distributions about the sensitive tissues (shielding materials and the astronaut's body) are important determining factors of the exposure levels and distributions of linear energy transfer. Local tissue environments during the SPE of September 29, 1989, with its HZE components are examined to analyze the importance of these ions to human SPE exposure. Typical space suit and lightly shielded structures leave significant contributions from HZE components to certain critical body tissues and have important implications on the models for risk assessment. A heavily shielded equipment room of a space vehicle or habitat requires knowledge of the breakup of these ions into lighter components, including neutrons, for shield design specifications.

14. SUBJECT TERMS	15. NUMBER OF PAGES
Shielding; Ionizing radiation; Heavy ions; Solar-particle event; Organ exposure	20
	16. PRICE CODE: A03

17. SECURITY CLASSIFICATION OF REPORT	18. SECURITY CLASSIFICATION OF THIS PAGE	19. SECURITY CLASSIFICATION OF ABSTRACT	20. LIMITATION OF ABSTRACT
Unclassified	Unclassified	Unclassified	UL

NSN 7540-01-280-5500

Standard Form 298 (Rev. 2-89)
Prescribed by ANSI Std. Z39-18
298-102